Many techniques for accomplishing this are now under investigation and will be reported in later articles.

ACKNOWLEDGMENT

The authors thank Dr. H. Lewis, Dr. H. Gerritsen and E. Sabisky of the RCA Laboratories in Princeton, N. J., for their many helpful discussions on the properties of rutile, and gratefully acknowledge the assistance of H. B. Yin, E. Denlinger and J. P. Laureillo with the maser measurements.

BIBLIOGRAPHY

[1] R. W. Degrasse, E. O. Schulz-Du Bois, and H. E. D. Scovil, "Three level solid state traveling-wave maser," *Bell Sys. Tech. J.*, vol. 38, pp. 305–334; March, 1959.
[2] H. D. Tenney, *et al.*, "An *S*-band traveling-wave maser," 1959, IRE WESCON CONVENTION RECORD, pt. 1, pp. 151–155.
[3] G. I. Haddad and J. E. Rowe, "*X*-band ladder-line traveling wave maser," IRE TRANS. ON MICROWAVE THEORY AND TECHNIQUES, vol. MTT-10, pp. 9–13; January, 1962.
[4] H. B. Yin, L. C. Morris, and D. J. Miller, "An *S*-band traveling-wave maser," PROC. IEEE (*Correspondence*), vol. 51, p. 225; January, 1963.
[5] D. J. Miller and H. B. Yin, "An *S*-band traveling-wave maser with a 30 per cent tunable bandwidth," PROC. IEEE (*Correspondence*) vol. 51, pp. 1779–1780; December, 1963.
[6] W. S. C. Chang, J. Cromack, and A. E. Siegman, "Cavity and Traveling Wave Masers Using Ruby at *S*-Band," Electronic Laboratories, Stanford University, Calif., Rept. No. 155-2; 1959.
[7] E. S. Sabisky and H. J. Gerritsen, "A traveling-wave maser using chromium-doped rutile," PROC. IRE (*Correspondence*), vol. 49, pp. 1329–1330; August, 1961.
[8] H. J. Gerritsen, S. E. Harrison, H. R. Lewis, and J. P. Wittke, "Chromium-doped Titania or a maser material," *Phys. Rev. Letters*, vol. 2, p. 153; 1959.
[9] E. S. Sabisky and H. J. Gerritsen, "Measurements of the dielectric constant of rutile (TiO_2) at microwave frequencies between 4.2° and 300° K," *J. Appl. Phys.*, vol. 33, pp. 1450–1453; April, 1962.
[10] P. N. Butcher, "The coupling impedance of tape structures," *J. Brit. IRE*, vol. 104, Pt. B, pp. 177–187; March, 1957.
[11] —— "A theoretical study of propagation along tape ladder lines," *J. Brit. IRE*, vol. 104, Pt. B, pp. 169–176; March, 1957.
[12] J. Clark and G. Harrison, "Miniaturized coaxial ferrite devices," *Microwave J.*, pp. 108–118; June, 1962.
[13] A. E. Siegman, Private correspondence and notes.

Coupled Circular Cylindrical Rods Between Parallel Ground Planes

EDWARD G. CRISTAL, MEMBER, IEEE

Summary—**The normalized self and mutual capacitances of periodic, circular cylindrical rods located between parallel ground planes are presented graphically. The capacitances were determined by solving the appropriate integral equation by numerical methods. Charts of self and mutual capacitance are given for rod diameter-to-ground plane spacing ratios varying from 0.05 to 0.8 and for very small to very large spacings between rods. Accuracy of the data is believed to be generally better than 2 per cent for the normalized mutual capacitance and generally better than 1 per cent for the normalized self capacitance. An approximate design method is also presented that permits using the data to synthesize filters (such as interdigital and comb-line filters) that require rods of nonequal diameters and spacings. An example of the design method is given, and a filter is constructed from the resulting data. The filter response was measured and found to agree closely with that called for by the theory.**

Manuscript received March 17, 1964. This work was sponsored by the U. S. Army Electronics Research and Development Agency, Fort Monmouth, N. J., under Contract No. DA 36-039-AMC-00084(E).

The author is with the Stanford Research Institute, Menlo Park Calif.

I. INTRODUCTION

THE DESIGN of many UHF and microwave filters is based on electrically coupling arrays of cylindrical bars located between parallel ground planes of which the comb-line and interdigital filter are two examples [1], [2]. In the past, rectangular bars generally have been used as coupling elements because the necessary data are available [3]. Filter equations and procedures of Matthaei [1], [2], together with design data of Getsinger [3], have been used to design filters which have proved to have excellent electrical characteristics. However, obtaining rectangular bars in practice requires manufacturing processes which are generally costly. On the other hand, the use of circular cylindrical rods as resonators offers several manufacturing advantages and should result in the same excellent electrical filter properties. For these reasons, design data of coupled circular cylindrical rods between parallel ground

planes and a design method for using the data to synthesize filters have been prepared and are presented in this paper.

The coupled rod data are presented in Section II. Also in Section II, the filter synthesis method is explained by means of an example. The mathematical derivation of the design data is given in Section III. The physical basis for the design method is presented in Section IV. A discussion of the accuracy of the coupled rod data will be found in Section V. The measured performance of a trial filter constructed from the design data of Section II is described in Section VI.

II. Technical Description

The geometry of the periodic, circular cylindrical rods between parallel ground planes and the dimensional notation are shown in Fig. 1. The circular rods have diameter d and are spaced periodically at a distance c. The ground planes are separated at distance b. The spacing between adjacent rod surfaces is denoted by s and is given by

$$s = c - d. \tag{1}$$

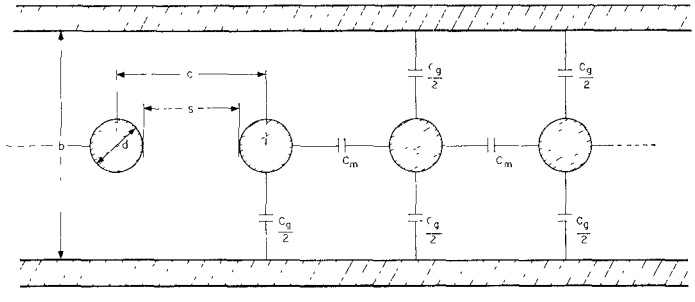

Fig. 1—Coupled circular cylindrical rods between parallel ground planes.

In the derivation of the design data fringing capacitances beyond nearest neighbors were neglected. It is therefore possible to describe TEM propagation along the structure in terms of two orthogonal modes which have been designated as the even mode and the odd mode. In the even mode all center conductors are at the same potential, while in the odd mode successive center conductors are at equal but opposite signed potentials with respect to the ground planes. These two TEM modes have different characteristic impedances which are intimately related to the total static capacitances of the rods to ground when in one or the other mode. The total static capacitances are related to the mutual capacitance between successive rods C_m and the self capacitance C_g of each rod. A consideration of Fig. 1 shows that the total capacitance measured between one rod and ground when the rods are driven in the odd mode is

$$C_0 = C_g + 4C_m, \tag{2}$$

and the total capacitance measured between one rod and ground when the rods are driven in the even mode is

$$C_e = C_g. \tag{3}$$

From (2) and (3) are obtained

$$C_g = C_e \tag{4}$$

and

$$C_m = 1/4(C_0 - C_e). \tag{5}$$

The characteristic impedance Z_0 of a lossless uniform transmission line operating in the TEM mode may be related to its shunt capacitance by

$$Z_0\sqrt{\epsilon_r} = \frac{\eta}{(C/\epsilon)} \text{ ohms} \tag{6}$$

where

ϵ_r is the relative dielectric constant of the medium in which the wave travels

η is the impedance of free space (376.7 ohms)

C/ϵ is the ratio of the static capacitance per unit length between conductors to the permittivity (in the same units) of the dielectric medium. (This ratio is independent of the dielectric constant.)

The even and odd mode impedances of coupled TEM lines can be found by substituting even and odd mode capacitances of the lines into (6).

Graphs of normalized capacitance C/ϵ vs normalized spacing s/b are presented in a form that assists the filter synthesis method. In Fig. 2, C_m/ϵ vs $(1/2)s/b$ is given. In Fig. 3, $(1/2)C_g/\epsilon$ vs $(1/2)s/b$ is given. Although these data are for the periodic structure of Fig. 1, a method has been developed whereby the data can be used for synthesis of filters in which rods of arbitrary diameters and spacings are required. The method is approximate, but is expected to give good results.

The design method will be explained by means of an example. To facilitate the evaluation of the method, a previously constructed interdigital band-pass filter that uses rectangular bars has been chosen as the example.[1] The filter design calls for a 6-resonator filter having a 10-per cent bandwidth and a 0.1-db Chebyshev ripple in the pass band. Because the filter is symmetrical about its center, only one-half the filter is shown in the cross-sectional view in Fig. 4, page 430. The nomenclature used in Fig. 4 is adopted for this discussion, except that the dimensions w_k and t for the rectangular cross section of the bars are replaced by the diameters d_k of the round rods. The required normalized capacitances for the design example are given in Table I [2].

[1] Matthaei, see [2], pp. 483–486.

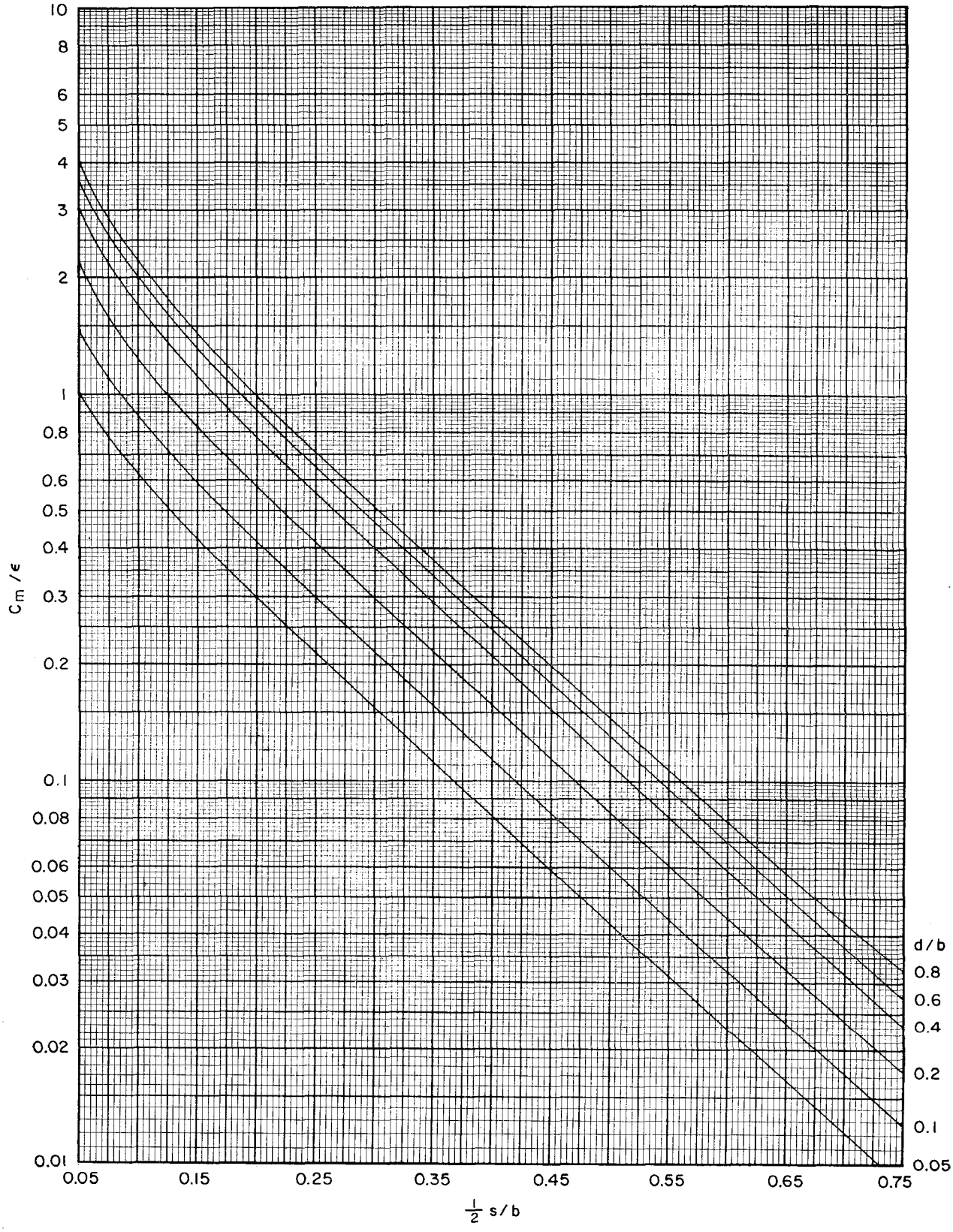

Fig. 2—Graph of C_m/ϵ (normalized mutual capacitance) vs $\frac{1}{2}(s/b)$ (normalized half spacing).

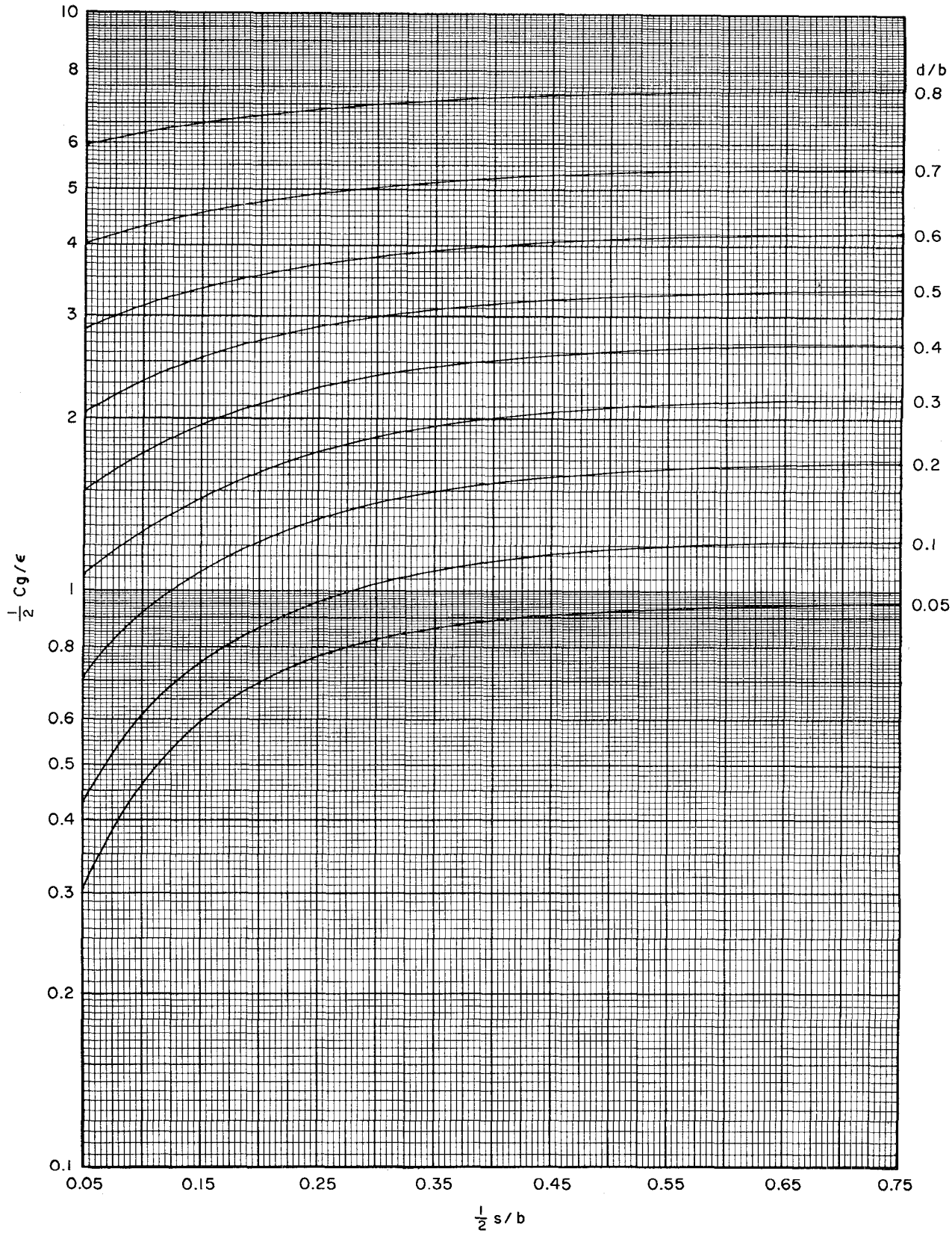

Fig. 3—Graph of $(\frac{1}{2})C_g/\epsilon$ (normalized half self capacitance) vs $(\frac{1}{2})s/b$ (normalized half spacing).

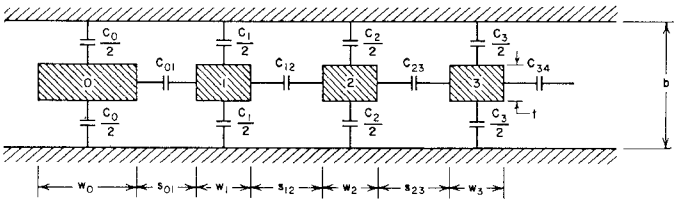

Fig. 4—Cross section of an array of parallel-coupled lines between ground planes.

TABLE I

TABULATION OF QUANTITIES OF A 10-PER CENT BANDWIDTH INTERDIGITAL FILTER DESIGN WITH $n=6$ RESONATORS [2]

k	$C_{k,k+1}/\epsilon$	k	C_k/ϵ
0 and 6	1.582	0 and 7	5.950
1 and 5	0.301	1 and 6	3.390
2 and 4	0.226	2 and 5	4.420
3	0.218	3 and 4	4.496

This filter was designed for 0.10-db Chebyshev ripple.

The design procedure given here assumes that values for the normalized capacitances have been previously obtained [1], [2]. The initial step in obtaining the dimensions of the structure from the normalized capacitances is to mark off on the graph of Fig. 2 horizontal lines corresponding to the values of C_m/ϵ that are called for in the design. In this example four horizontal lines of $C_m/\epsilon = C_{k,k+1}/\epsilon$ (for $k=0, 1, 2, 3$) $=1.58$, 0.301, 0.226, and 0.218 are drawn. Next, the coordinates of the intersections of constant $C_m/\epsilon=0.218$, 0.226, 0.301, and 1.58 with the family of constant d/b curves are noted and plotted on the graph of Fig. 3. Smooth curves are then drawn on the graph of Fig. 3 through points of constant C_m/ϵ, thus obtaining curves of constant C_m/ϵ. This is shown in Fig. 5.

Next, it is useful to partition the filter configuration of Fig. 4 into smaller subsections as shown in Fig. 6. Each subsection consists of a normalized capacitance to ground and the normalized coupling capacitances to the right and to the left. To determine the normalized rod diameters and normalized spacings the designer may choose any of the subsections (a), (b), (c) or (d) of Fig. 6 and proceed in the following manner: Assume that Fig. 6(d) is chosen. On the graph of Fig. 5, assisted by a suitable drawing aid, several auxiliary curves of constant d/b are drawn which intersect the curves of constant $C_m/\epsilon=0.218$ and 0.226. These auxiliary curves are drawn in the vicinity of one-half the value of the required normalized capacitance to ground, in this case, $(1/2)C_g/\epsilon=(1/2)C_3/\epsilon=2.25$. *The objective of drawing auxiliary curves is to find the unique intersections with the constant curves of $C_m/\epsilon=0.218$ and 0.226 such that the sum of the ordinates of the intersections totals $C_g/\epsilon=C_3/\epsilon=4.5$.* The proper d/b curve is shown in Fig. 7.

It is seen in Fig. 7 that the coordinates of the intercept at $C_m/\epsilon=0.218$ are $[(1/2)s/b=0.387$, $(1/2)C_g/\epsilon=2.25]$, and those at $C_m/\epsilon=0.226$ are (0.381, 2.25). Note that the sum of the ordinates is 4.5 as required. Next, using linear interpolation, d/b of rod 3 is found to be 0.351.

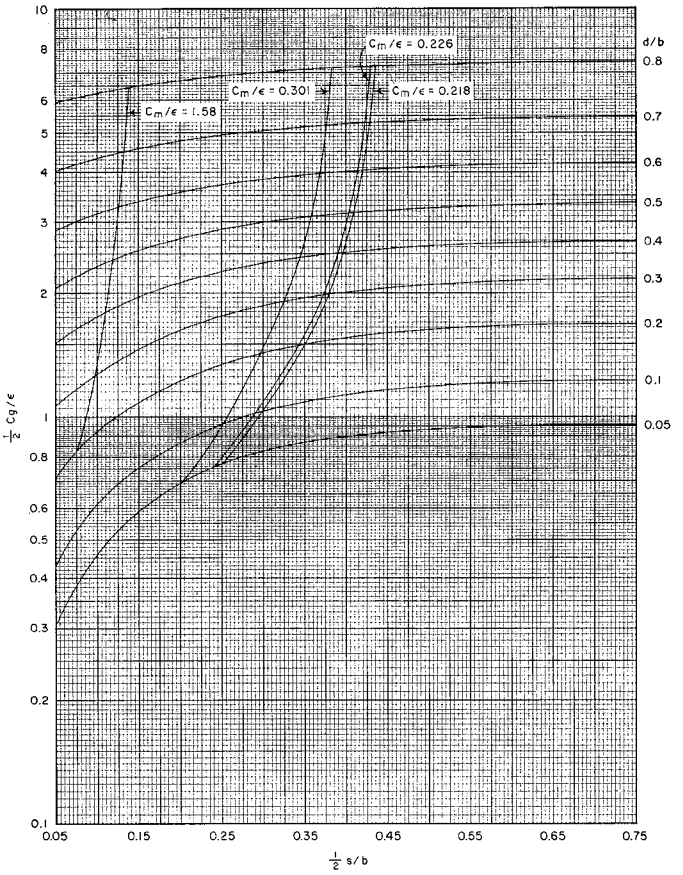

Fig. 5—Curves of constant C_m/ϵ plotted on a graph of $(\frac{1}{2})C_g/\epsilon$ vs $(\frac{1}{2})$ s/b.

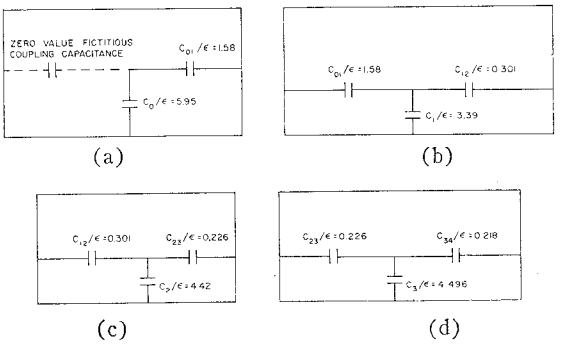

Fig. 6—Groupings of self and mutual capacitances used in the design example.

Next, the same technique is applied to the values of normalized capacitance in Fig. 6(c). The correct auxiliary curve of constant d/b is shown in Fig. 8, in which the coordinates of the intercepts with $C_m/\epsilon=0.226$ and 0.301 are (0.381, 2.24) and (0.335, 2.18), respectively. Note that the ordinates of the intercepts are unequal; this will usually be the case. However, the sum of the ordinates must equal the normalized capacitance to ground. In this case the sum of the ordinates is $2.24+2.18=4.42=C_2/\epsilon$. By linear interpoltion d/b of rod 2 is found to be 0.352.

Proceeding to Fig. 6(b) and again applying the design technique, it is found that the coordinates of the intercepts of the auxiliary constant d/b curve with the $C_{12}/\epsilon=0.301$ and $C_{01}/\epsilon=1.582$ curves are (0.330, 2.03) and (0.098, 1.36), respectively. The d/b of rod 1 is found by linear interpolation to be 0.324.

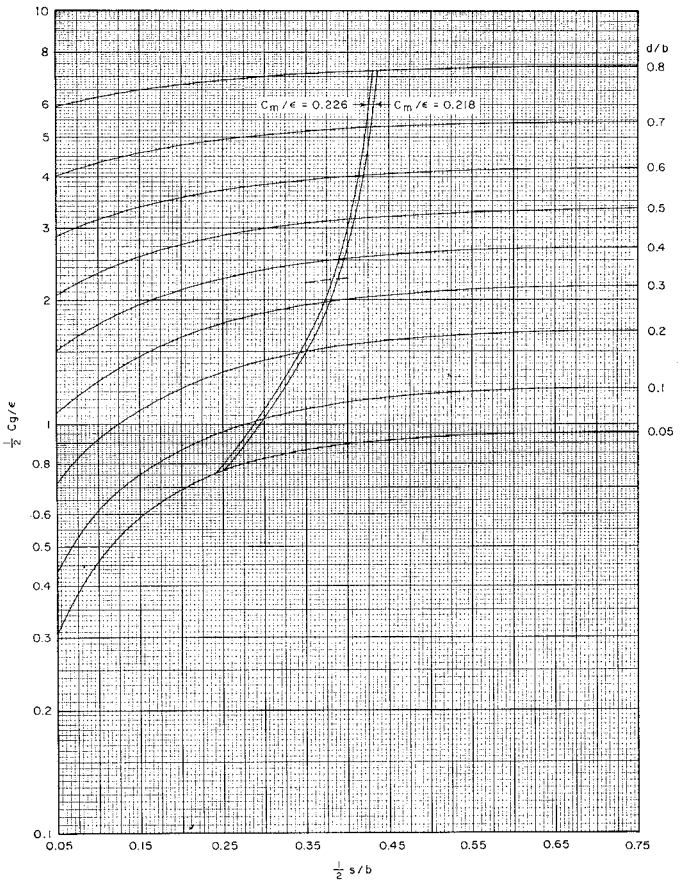

Fig. 7—Determination of the normalized diameter of rod 3 and the partial spacings to rods 2 and 4.

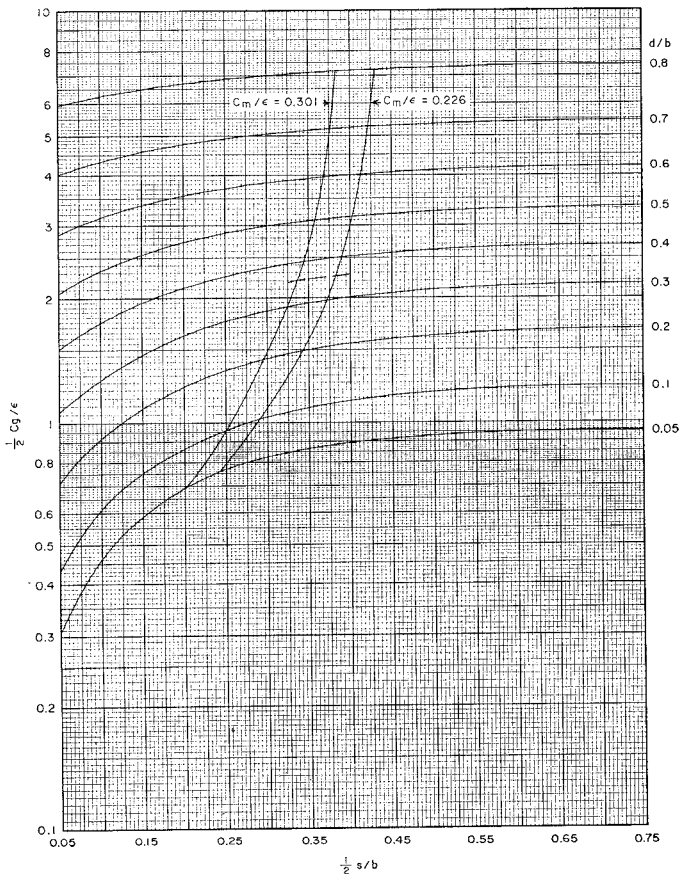

Fig. 8—Determination of the normalized diameter of rod 2 and the partial spacings to rods 1 and 3.

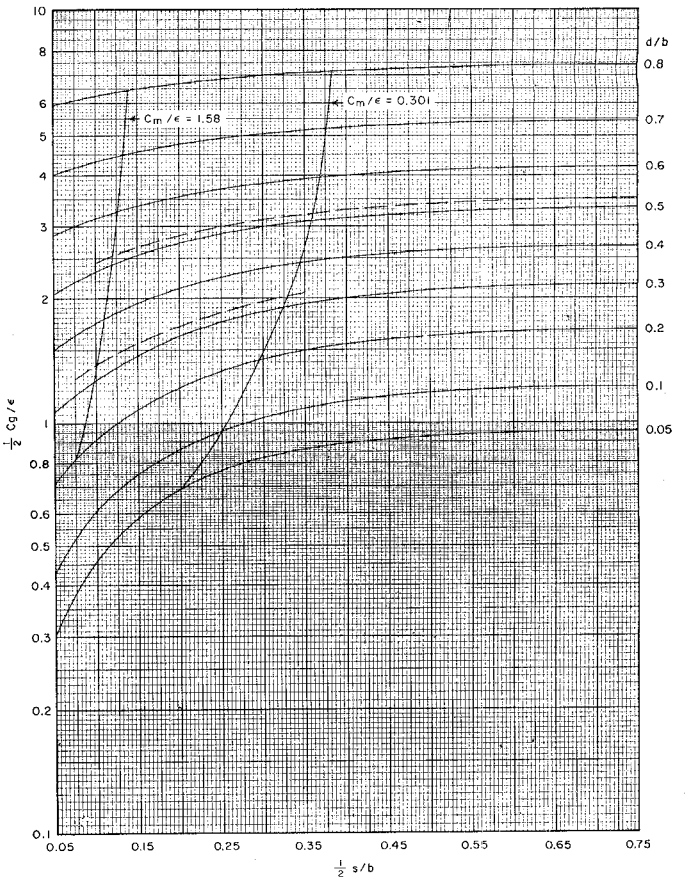

Fig. 9—Determination of the normalized diameter of rods 0 and 1, and the respective partial spacings to adjacent rods.

Finally, the design technique is applied to Fig. 6(a), and the coordinates (0.120, 2.5) are determined as the intercept of the auxiliary constant d/b curve and the $C_{01}/\epsilon = 1.582$ curve. The coordinates (∞, 3.45) are found as the intercept of the same constant d/b curve with the fictitious coupling capacitance to the left of C_0 set equal to zero. In the latter instance the right-hand extreme of Fig. 5 is used where the constant d/b curves are virtually flat. By linear interpolation, d/b of rod 0 is found to be 0.516. The auxiliary constant d/b curves used in the last two subsections are shown in Fig. 9.

The respective normalized spacings, $s_{k,k+1}/b$ are obtained by summing abscissa values that correspond to the same mutual capacitance. Bookkeeping is simplified by placing abscissa values along their corresponding mutual capacitances:

Abscissa Value, $(1/2)s/b$	$C_{k,k+1}$	Obtained From
0.120	C_{01}	Fig. 6(a)
0.098 0.330	C_{01} C_{12}	Fig. 6(b)
0.335 0.381	C_{12} C_{23}	Fig. 6(c)
0.381 0.387	C_{23} C_{34}	Fig. 6(d)

Therefore,

$$s_{01}/b = 0.120 + 0.098 = 0.218 = s_{67}/b$$
$$s_{12}/b = 0.330 + 0.335 = 0.665 = s_{56}/b$$
$$s_{23}/b = 0.381 + 0.381 = 0.762 = s_{45}/b$$
$$s_{34}/b = 0.387 + 0.387 = 0.774.$$

Center to center spacings may be obtained by adding to the appropriate s/b value $(1/2)d/b$ of the rod on the left and $(1/2)d/b$ value of the rod on the right.

Thus,

$$c_{k,k+1}/b = s_{k,k+1}/b + (1/2)d_k/b + (1/2)d_{k+1}/b$$
$$c_{01}/b = 0.218 + 0.258 + 0.162 = 0.638 = c_{67}/b$$
$$c_{12}/b = 0.665 + 0.162 + 0.176 = 1.003 = c_{56}/b$$
$$c_{23}/b = 0.762 + 0.176 + 0.175 = 1.114 = c_{45}/b$$
$$c_{34}/b = 0.774 + 0.1755 + 0.1755 = 1.125.$$

The normalized rod diameters obtained as described previously using Figs. 7–9 are

$$d_0/b = 0.516 = d_7/b$$
$$d_1/b = 0.324 = d_6/b$$
$$d_2/b = 0.352 = d_5/b$$
$$d_3/b = 0.351 = d_4/b.$$

The design specifications for the filter using rectangular bars and the same filter using round rods are compared in Table II, where the spacings between successive round rods are closer, in general, than spacings between successive rectangular bars. Also, the round rods are larger in cross-sectional areas than the rectangular bars.

TABLE II

PARAMETERS OF AN INTERDIGITAL FILTER DESIGN USING ROUND RODS COMPARED WITH THE SAME FILTER USING RECTANGULAR BARS

k	Round Rods	Rectangular Bars	k	Round Rods	Rectangular Bars	Rectangular Bars
	$s_{k,k+1}/b$	$s_{k,k+1}/b$		$(d/b)_k$	$(w/b)_k$	$(t/b)_k$
0 and 6	0.218	0.255	0 and 7	0.516	0.648	0.3
1 and 5	0.665	0.670	1 and 6	0.324	0.243	0.3
2 and 4	0.762	0.820	2 and 5	0.352	0.294	0.3
3	0.774	0.830	3 and 4	0.351	0.293	0.3

III. Mathematical Determination of C_m and C_q

The boundary-value problems associated with the periodic cylindrical rods between parallel ground planes depend on the mode of excitation. When the structure is excited in the odd mode the mathematical problem is to satisfy Laplace's equation in the region shown in Fig. 10(a), and the boundary conditions as given in the figure. This is a Dirichlet problem. When the structure is excited in the even mode the mathematical problem is to satisfy Laplace's equation in the region shown in Fig. 10(b) and the boundary conditions as shown in this figure. This is a boundary-value problem with mixed boundary conditions.

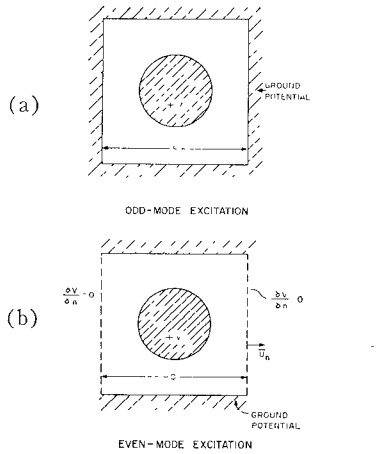

Fig. 10—Equivalent boundary value problems associated with the even and odd mode excitation of the coupled circular rods.

As stated in Section II, the capacitance associated with the solution of the Dirichlet problem is given by (2), and the capacitance associated with the solution of the mixed boundary problem is given by (3). From these are obtained C_m and C_q.

The method of determining the even and odd mode capacitances was to solve the integral equation associated with the boundary-value problem and thus obtain the normalized surface charge density; then the total normalized charge was obtained by integration. The normalized charge was divided by the potential difference to give the normalized capacitance. The generalized integral equation for both boundary-value problems is

$$V(\bar{r}_0) = -\frac{1}{2\pi}\oint_P \left[\frac{\eta(\bar{r})}{\epsilon}\right] \ln|\bar{r} - \bar{r}_0|\, ds(\bar{r}) + \frac{1}{2\pi}\oint_P V(\bar{r}) \frac{\bar{u}_r \cdot \bar{u}_n}{|\bar{r} - \bar{r}_0|}\, ds(\bar{r}) + \frac{1}{2} V(\bar{r}_0) \quad (7)$$

wherever the boundary curve has a unique tangent.[2] P denotes the principal value of the integral.[3]

[2] In Fig. 11, it is shown that the path of integration for (7) has an interior right angle. If the position vector $\bar{r}_0$ lies at this point, the term $(1/2)V(\bar{r}_0)$ on the right-hand side of (7) should be replaced by $(3/4)V(r_0)$.

[3] Eq. (7) may be derived by taking the two-dimensional integral formulation for the potential at a point within a closed boundary and permitting the observation point to approach the boundary (See, for example, J. A. Stratton, "Electromagnetic Theory," McGraw-Hill Book Co., Inc., New York, N. Y., pp. 166–170 and problem 8, p. 219; 1941), and permitting the observation point ot approach the boundary. The limiting operation may be performed as in Mai and Van Bladel [11], or alternatively, the observation point may alternatively be placed on the boundary and the boundary curve in the vicinity of the observation point deformed into an appropriate segment of a circle of infinitesimally small radius. The deformation is such as to leave the observation point within the boundary. The segment of circle is π radians where the boundary curve has a unique tangent and is $\frac{3}{2}\pi$ radians at the right angle.

For the Dirichlet problem (7) reduces to

$$0 = \oint_P \left[\frac{\eta(\bar{r})}{\epsilon}\right] \ln \left| \bar{r} - \bar{r}_0 \right| ds(\bar{r})$$

on the outer boundary

$$-2\pi(V_i - V_o) = \oint_P \left[\frac{\eta(\bar{r})}{\epsilon}\right] \ln \left| \bar{r} - \bar{r}_0 \right| ds(\bar{r})$$

on the inner boundary (8)

where V_i and V_o are the respective potentials on the inner and the outer boundary. The notation used in (7) and (8) is clarified by Fig. 11. Vector $\bar{r}$ is a position vector from an arbitrary origin to a point on the boundary at which the integrand is being evaluated. Vector $\bar{r}_0$ is a position vector to a point on the boundary where the voltage is being evaluated. Voltages $V(r)$ and $V(\bar{r}_0)$ are the voltages at the vector positions $\bar{r}$ and $\bar{r}_0$, respectively. Vector $\bar{u}_r$ is a unit vector in the direction of $\bar{r} - \bar{r}_0$. Vector $\bar{u}_n$ is the outward pointing unit normal to the boundary surface. Finally, $ds(\bar{r})$ is the differential length of the boundary curve at the vector position $\bar{r}$, and $\eta(\bar{r})/\epsilon$ is the normalized surface charge density at the vector position $\bar{r}$.

The method of solution was to divide the boundary curve into n subintervals, and assign to each subinterval an unknown constant normalized surface charge density or an unknown constant potential. These unknown constants were then removed from under the integral sign and the integrations performed analytically or numerically in each subinterval. In the general case, (7) takes the form

$$V(\bar{r}_i) = \frac{1}{2\pi} \sum_{j=1}^{n} \left\{ -\frac{\eta(\bar{r}_j)}{\epsilon} \int_{\text{subinterval } j} \ln \left| \bar{r}_j - \bar{r}_i \right| ds(\bar{r}_j) + V(\bar{r}_j) \int_{\text{subinterval } j} \frac{\bar{u}_r \cdot \bar{u}_n}{\left| \bar{r}_j - \bar{r}_i \right|} ds(\bar{r}_j) \right\} + \left(\frac{1}{2}\right) V(\bar{r}_i) \quad (9)$$

for $i = 1, 2, \cdots, m$. Because of the symmetry of the boundary curve and boundary conditions, (9) may be reduced by a factor of 4 or, alternatively, the problem may be reformulated using one quadrant of the structure. (The former procedure was used in this work.) After the integrations in (9) had been carried out, the equations were arranged into a matrix. For (8) the matrix takes the form

$$\begin{pmatrix} 0 \\ 0 \\ \cdot \\ \cdot \\ \cdot \\ V \\ V \\ \cdot \\ \cdot \\ \cdot \\ V \end{pmatrix} = \begin{pmatrix} g_{11} & g_{12} \cdots g_{1n} \\ g_{21} & \cdots g_{2n} \\ & \\ \cdot & \cdot \\ \cdot & \cdot \\ \cdot & \cdot \\ & \\ & \\ g_{m1} & g_{mn} \end{pmatrix} \begin{pmatrix} \eta_1/\epsilon \\ \eta_2/\epsilon \\ \\ \cdot \\ \cdot \\ \cdot \\ \\ \\ \eta_m/\epsilon \end{pmatrix} \quad (10)$$

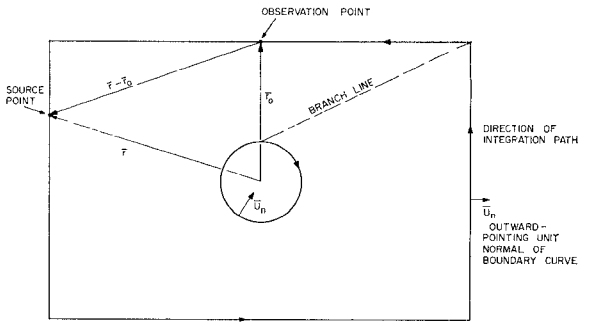

Fig. 11—Geometry and vector nomenclature used in the even and odd mode boundary value integral equation.

where V is the potential difference between the boundaries. For (7), the matrix takes the form

$$\begin{pmatrix} \tilde{V}_1 \\ \tilde{V}_2 \\ \cdot \\ \cdot \\ \cdot \\ \\ \\ \tilde{V}_m \end{pmatrix} = \begin{pmatrix} G_{11} & G_{12} \cdots G_{1n} \\ G_{21} & \cdots G_{2n} \\ & \\ \cdot & \cdot \\ \cdot & \cdot \\ \cdot & \cdot \\ & \\ & \\ G_{m1} & G_{mn} \end{pmatrix} \begin{pmatrix} \eta_1/\epsilon \\ \cdot \\ \cdot \\ \eta_s/\epsilon \\ V_1 \\ \cdot \\ \cdot \\ V_r \end{pmatrix} \quad (11)$$

where V_i $(i = 1, 2, \cdots, r)$ represents the unknown potential on the part of the boundary where $\partial V/\partial n = 0$; and $\tilde{V}_i$ $(i = 1, 2, \cdots, m)$ are constants which take into account contributions from the second term on the right in (7). The entries g_{ij} and G_{ij} are constants obtained from the indicated integrations in (9).

In solving (10) and (11) it was found that convergence was quicker in many cases when an overdetermined set of equations was compiled (*i.e.*, $m > n$) and a least squares method used to solve them [4]. This was done in all cases. In order to guarantee accuracy of the inverted matrix, which was generally a 40 by 40 matrix, perturbation methods were used which required the inverse matrix to be accurate to 0.01 per cent [5]. This was found necessary because of the loss of significant digits in inverting the very large matrices in (10) and (11).

In order to determine whether or not a solution to (10) or (11) gave a sufficiently close approximation to the even or odd mode capacitance, the number of subintervals of the boundary curve was increased, thereby increasing the number of simultaneous equations. The capacitance obtained from the solution of the new set of equations was next compared with that of the former set. When the capacitance remained sufficiently invariant to successive enlargements of the matrix, convergence was assumed.[4] In order to avoid having to test every solution by this method, several geometries were picked that appeared to offer the greatest difficulty of obtaining convergence. The largest order that was required to obtain convergence for these geometries was used for all subsequent cases.

[4] The problem of convergence and of the accuracy of the solutions will be discussed in Section V.

One additional refinement was explored in attempting to obtain fast convergence. The side condition that the total charge be zero was attached, although the condition is redundant in that it is satisfied by the proper solution. This technique was applied only to (11). In the few cases examined, the additional side condition did appear to result in a better approximation to the correct answer with smaller matrices than the former method without side conditions. However, for large matrices no general trend was clear. Also for rods of very small diameter (*i.e.*, $d/b<0.3$), the inverse matrix of (11) could not be obtained in the time allowed. This inability to obtain an inverse matrix was probably due to the side condition making the matrix of (11) extremely skew [6] and thereby causing too great a loss of significant digits when the matrix was inverted.

IV. Physical Basis for the Method of Designing Filters that Use Rods of Unequal Diameters and Spacings

Fig. 12 shows three rods of a hypothetical multirod filter configuration with the self capacitances divided into left and right components parts. The following assumptions are made concerning the coupled-rod configuration.

1) Coupling beyond nearest neighbors is negligible.
2) A moderate change in the size or spacing of a given rod has only a second-order effect on the charge distribution on the far side of adjacent rods.

Therefore, by assumptions 1) and 2), the mutual capacitance $C_{i,i+1}$ is dependent only on the right half of rod i and the left half of $i+1$, and (from Fig. 12) C_i^L is independent of the spacing and diameter of the adjacent rod on the right; C_i^R is independent of the spacing and diameter of the adjacent rod on the left. The self capacitance of a rod is given by

$$C_i = C_i^L + C_i^R. \tag{12}$$

Consider the rods in Fig. 12 to be excited in the odd mode. This is shown in Fig. 13 where the electric flux lines are sketched and a ground value equipotential line is approximated. The equipotential line will be approximately straight for rods having moderate and far spacings and should not be strongly dependent on the rod diameters with these spacings. (In most filter designs the rods in the center of the filter are nearly the same diameter and only vary greatly at the ends of the filter.) If the rods were excited in the even mode, then the equipotential line in Fig. 13 would approximately be the line where, also, $\partial V/\partial n=0$.[5]

Again from Fig. 13, it may be stated on the basis of the previous approximations that the left half of rod 2 sees boundary conditions which are equivalent to a system of equispaced, equidiameter rods of diameter d_2 spaced at $s=s_2^L$ and having a mutual capacitance

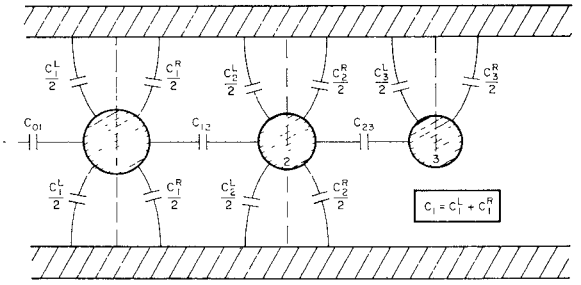

Fig. 12—Hypothetical multirod filter configuration showing division of self capacitance into left and right component parts.

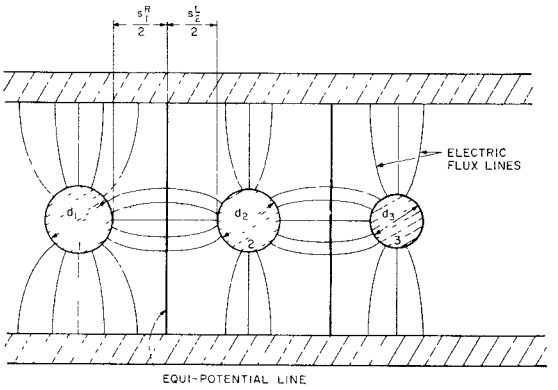

Fig. 13—Hypothetical multirod filter configuration excited in odd mode.

$C_m=C_{12}$. (Note that $s_2^L/2$ is indicated in Fig. 13.) At the same time, the right half of rod 1 sees boundary conditions equivalent to a system of equispaced, equidiameter rods of diameter d_1 spaced at $s=s_1^R$ but also with a mutual capacitance of $C_m=C_{12}$.[6] Through the use of this artifice (*i.e.*, approximating left and right boundary conditions independently) the designer is able to use the data given in Figs. 2 and 3 to obtain arbitrary values of mutual and self capacitance needed in a filter design. The design method described in Section II is one method of utilizing the above artifice. The method described was found easy to apply and also efficient in terms of design time.

V. Accuracy of the Solutions

A difficulty that arises from solving (7) and (8) by the method discussed in Section III is that the accuracy of the solution cannot be precisely stated. Although other methods of solutions are possible which in theory give upper and lower bounds for the answer [7] (at least in the Dirichlet problem), practical considerations make these methods undesirable in this particular problem. However, in order to be sure of the results obtained by the method of Section III, several comparisons are made in Table III with data taken from other sources.

By replacing the round rods with infinitesimal line charges located at the center of each cylinder and using the method of images, a solution has been obtained

[5] This approximation is perhaps in error more than previous approximations. However, for moderately spaced rods the even mode capacitance is not strongly dependent on spacing. Therefore, a larger error in the position of the $\partial V/\partial n=0$ line can be tolerated.

[6] This concept (*i.e.*, that the proper left and right half spacings are determined when successive rods have the same mutual capacitance) is credited to Dr. G. L. Matthaei.

TABLE III

COMPARISONS OF CHARACTERISTIC IMPEDANCES OBTAINED FROM SOLUTIONS OF (7) AND (8) WITH THOSE OBTAINED FROM PUBLISHED SOURCES

Case		Z_{even} ohms This Work	ITT-Handbook [8]* $Z_{even}=138\log_{10}[(4/\pi)/(d/b)]$ Accuracy not specified	Per cent Difference
d/b	s/b			
0 6	1.5	44.1	45.1	1.5 per cent
0.4	1.5	68.7	69.4	1.0 per cent
0.2	1.5	109.8	110.9	0.99 per cent
Case		Z_{odd} ohms This Work	ITT-Handbook [9]** Z_{odd} ohms Accuracy not specified	Per cent Difference
d/b	s/b			
0.5	0.5	46.1	45.0	2.5 per cent
0.1	0.9	142.6	141.5	0.78 per cent
Case		Z_{odd} ohms This Work	Chisholm [10]*** Z_{odd} ohms Accuracy about 0.6 per cent, when the impedance is of the order of 50 ohms.	Worst Per cent Difference
d/b	s/b		Min — Max	
0.8	1.5	25.2	25.26 — 25.86	2.31 per cent
0.6	1.5	44.1	44.25 — 44.40	0.68 per cent

* The case here is for a single wire between parallel ground planes which is similar to the case of widely spaced coupled rods excited in even mode.

** The case here is for a single wire centered in a square waveguide which is equivalent to the odd mode case wherein $d/b+s/b=1$.

*** The case here is the trough line; wide spacing is used to make the comparison practical.

which gives the correct asymptotic form to the solutions of the actual round-rod problems in the even and odd mode. A second-order correction to the solution was made which gives the following equations for the even and odd mode normalized capacitance:

$$\frac{\epsilon}{C_{odd}}=\frac{1}{2\pi}\left|\ln\frac{\frac{\pi}{4}\frac{d}{b}}{\sqrt{1-\left(\frac{d}{2b}\right)^4}}-\frac{1}{2}\ln\left[1-\left(\frac{d/b}{2(c/b)}\right)^4\right]+2\sum_{m=1}^{\infty}(-1)^m\ln\tanh m\frac{\pi}{2}\frac{c}{b}\right| \quad (13)$$

$$\frac{\epsilon}{C_{even}}=\frac{1}{2\pi}\left|\ln\frac{\frac{\pi}{4}\frac{d}{b}}{\sqrt{1-\left(\frac{d}{2b}\right)^4}}+\frac{1}{2}\ln\left[1-\left(\frac{d/b}{2(c/b)}\right)^4\right]+2\sum_{n=1}^{\infty}\ln\tanh m\frac{\pi}{2}\frac{c}{b}\right|. \quad (14)$$

These equations should be quite accurate for small d/b, say $d/b<0.3$, and $c/b>3(d/b)$. Table IV shows a comparison of C_g/ϵ and C_m/ϵ obtained from (13) and (14) with those obtained from the method in Section III.

In conclusion, the number and consistency of very good checks indicates that the accuracy of C_m/ϵ and G_g/ϵ obtained from the numerical solutions of (7) and (8) is generally better than 2 and 1 per cent, respectively.

TABLE IV

COMPARISON OF NORMALIZED CAPACITANCES OBTAINED FROM (13) AND (14) WITH THOSE OBTAINED FROM SOLUTIONS OF (7) AND (8)

d/b	s/b	Per Cent Difference Mutual Capacitances	Per Cent Difference Self Capacitances
0.4	0.40	2.43	1.60
	0.50	2.68	1.08
	0.70	2.83	0.53
	0.90	2.77	0.30
	1.20	2.46	0.16
	1.50	3.82	0.16
0.2	0.20	0.06	1.057
	0.30	0.17	0.01
	0.40	0.72	0.64
	0.50	0.39	0.21
	0.70	1.50	0.40
	0.90	1.28	0.16
	1.20	1.21	0.04
	1.50	1.22	0.01
0.1	0.20	0.07	0.12
	0.30	0.06	0.08
	0.40	0.26	0.30
	0.50	1.01	0.64
	0.70	2.06	0.58
	0.90	1.22	0.14
	1.20	1.06	0.05
	1.50	1.09	0.01
0.05	0.10	0.52	0.54
	0.15	0.12	0.204
	0.20	0.02	0.13
	0.30	0.03	0.08
	0.40	0.16	0.14
	0.50	0.59	0.33
	0.70	3.55	0.87
	0.90	1.33	0.17
	1.20	1.09	0.01
	1.50	1.03	0.02

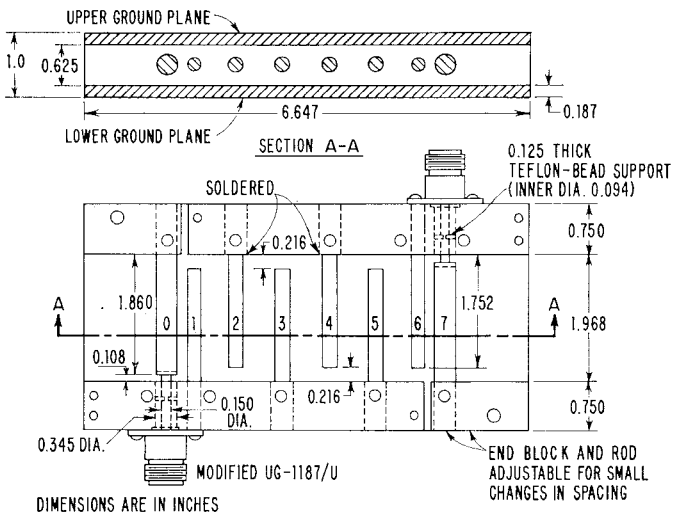

TOP VIEW, UPPER GROUND PLANE REMOVED

ROD DIAMETERS AND CENTER TO CENTER SPACING IN INCHES

K	DIAMETER OF ROD K	K	CENTER TO CENTER SPACING ($C_{K,K+1}$) OF RODS K AND K+1
0 AND 7	0.322	0 AND 6	0.399*
1 AND 6	0.200	1 AND 5	0.627
2 AND 5	0.220	2 AND 4	0.696
3 AND 4	0.219	3	0.703

* ADJUSTED TO 0.391 IN FINAL STRUCTURE

Fig. 14—Drawing of interdigital filter using round rods.

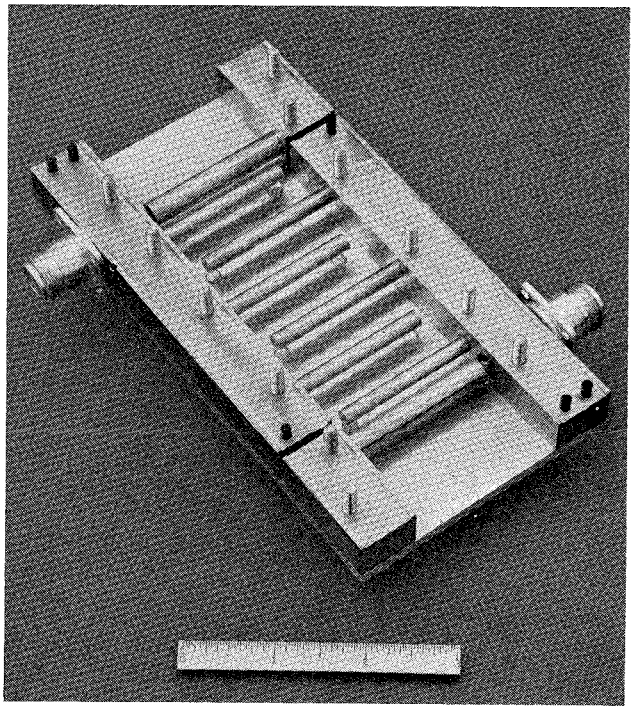

Fig. 15—Photograph of a trial interdigital filter using round rods.

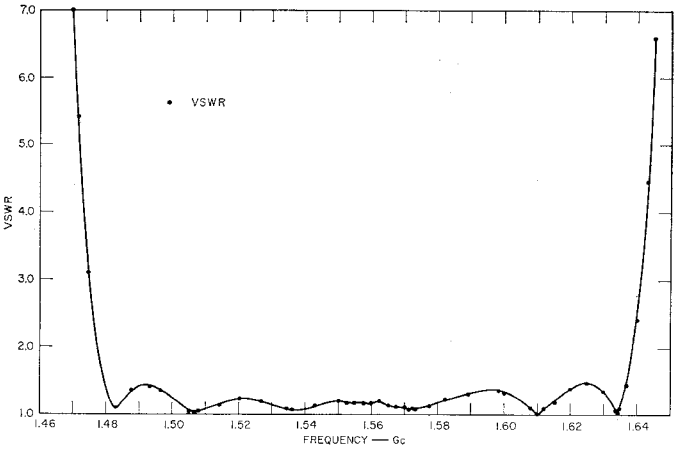

Fig. 16—Measured VSWR of interdigital filter using round rods.

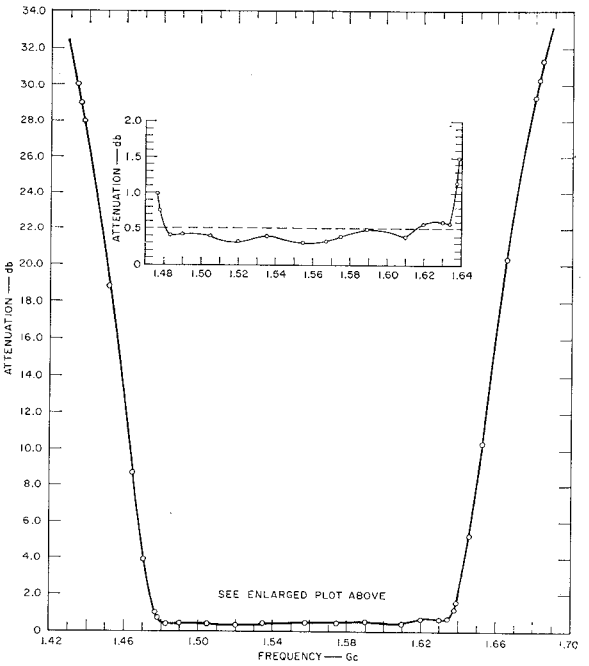

Fig. 17—Measured attenuation of interdigital filter using round rods.

VI. Trial Interdigital Filter

The interdigital filter whose design was described in Section II was constructed with $\frac{5}{8}$-inch ground-plane spacing and design center frequency of 1.5 Gc. Previous work with interdigital filters using rectangular bars showed that the spacing between the end resonators and the impedance-transforming section (*i.e.*, rods 0 and 1 and rods 6 and 7 in the present case) should be adjustable for small changes in spacing [2]. Therefore, the filter was constructed accordingly. A drawing of the filter is given in Fig. 14, and a photograph of the constructed filter is given in Fig. 15.

When the filter was initially tested, the pass band VSWR was slightly high. This condition was corrected by reducing the spacing between the terminations and

the first resonator on each end (*i.e.*, s_{01} and s_{67}) by about 0.008 inch—or about 6 per cent. The resulting VSWR is shown in Fig. 16. It is seen to be very nearly Chebyshev although the ripple peaks near the band edge are slightly high. (A 0.1-db Chebyshev ripple calls for VSWR peaks of 1.36.)

Fig. 17 shows the measured attenuation characteristic of the filter. The measured fractional bandwidth is 0.0996 which is very near the design value of 0.10. (With rectangular bars, the same filter design has a measured fractional bandwidth of 0.0935, a shrinkage of 7 per cent in bandwidth [2].) The shift of the center frequency of the filter to 1.557 results from the resonators being slightly short, as noted by Matthaei [2].

VII. Conclusions

The normalized self and mutual capacitances of periodic, circular cylindrical rods located between parallel ground planes were given graphically. The capacitances were determined by solving the appropriate integral equation by numerical methods. Data were presented for rod diameter-to-ground-plane spacing ratios varying from 0.05 to 0.8 for very near to very far rod spacings. Accuracy of the data is believed to be generally better than 2 per cent for the normalized mutual capacitance, and generally better than 1 per cent for the normalized self capacitance.

An approximate design method was also presented which permits using the data to synthesize filters that require rods of nonequal diameters and spacings. The design method should be most reliable for moderately and far spaced rods, but it should also be suitable for more closely spaced rods. (Closely spaced rods would probably require some experimental adjustments.)

An example of the design method was given. The relative rod diameters and spacings were determined for a 10-per cent 6-resonator 0.1-db Chebyshev ripple, interdigital filter. This design was constructed and tested, and its performance was found to conform closely to that called for by theory, thus tending to confirm the accuracy of the design data and the validity of the design method. Using round rods rather than rectangular bears in filters where these types of resonators are required (such as in comb-line and interdigital filters) should reduce manufacturing cost while retaining the electrical characteristics of the filter.

Acknowledgment

The computer programming of Stanford University's IBM 7090 computer for the computation of the data for the design of round rods between parallel ground planes was done by P. H. Omlor.

Robert Pierce fabricated the interdigital filter described in this paper, and York Sato made the laboratory tests.

Dr. G. L. Matthaei proposed a way of adapting the periodic, coupled-rod data to synthesis of filters that require arbitrary rod diameters and spacings. The author is indebted to him for his contribution to this paper and also for other helpful suggestions made during the course of this work.

References

[1] G. L. Matthaei, "Comb-line band-pass filters of narrow or moderate bandwidth," *Microwave J.*, vol. 6, pp. 82–96; August, 1963.
[2] G. L. Matthaei, "Interdigital band-pass filters," IRE Trans. on Microwave Theory and Techniques, vol. MTT-10, pp. 479–491; November, 1962.
[3] W. J. Getsinger, "Coupled rectangular bars between parallel plates," IRE Trans. on Microwave Theory and Techniques," vol. MTT-10, pp. 65–72; January, 1962.
[4] C. Lanczos, "Applied Analysis," Prentice-Hall, Inc., Englewood Cliffs, N. J., pp. 156–161; 1956.
[5] *Ibid.*, p. 148.
[6] *Ibid.*, pp. 161–163.
[7] H. J. Greenberg, "The determination of upper and lower bounds for the solution of the Dirichlet problem," *J. Math. and Phys.*, vol. 27, pp. 161–181; July, 1948.
[8] "Reference Data for Radio Engineers," International Telephone and Telegraph Corp., American Book-Stratford Press, Inc., New York, N. Y., 4th Edition, ch. 20, Part P, p. 592; 1956.
[9] *Ibid.*, ch. 20, p. 590, Part H.
[10] R. M. Chisholm, "The characteristic impedance of trough and slab lines," IRE Trans. on Microwave Theory and Techniques, vol. MTT-4, pp. 166–172; July, 1956.
[11] K. K. Mei, J. G. Van Bladel, "Scattering by perfectly-conducting rectangular cylinders," IEEE Trans. on Antennas and Propagation, vol. AP-11, pp. 191–192; March, 1963.